

Supplementary Materials: A Cancer Stem Cell Potent Cobalt(III)–Cyclam Complex Bearing Two Tolfenamic Acid Moieties

Paul B. Cressey, Arvin Eskandari and Kogularamanan Suntharalingam

Table of Content

- Figure S1** ^1H NMR spectrum in $\text{DMSO}-d_6$ of the cobalt(III)–cyclam complex, **3**.
Figure S2 ^{13}C NMR spectrum in $\text{DMSO}-d_6$ of the cobalt(III)–cyclam complex, **3**.
Figure S3 ESI-TOF mass spectrum (positive mode) of the cobalt(III)–cyclam complex, **3**.
Figure S4 ^1H NMR spectrum in $\text{DMSO}-d_6$ of tolfenamic acid.
Figure S5 UV–vis spectrum of **3** (25 μM) in PBS over the course of 24 h at 37 $^\circ\text{C}$.
Figure S6 UV–vis spectrum of **3** (25 μM) in PBS in the presence of ascorbic acid (250 μM) over the course of 24 h at 37 $^\circ\text{C}$.
Figure S7 UV–vis spectrum of tolfenamic acid (25 μM) in PBS at 37 $^\circ\text{C}$.
Figure S8 ESI-TOF mass spectrum (positive mode) of **3** (25 μM) in PBS, in the presence of glutathione (250 μM) after 72 h.
Figure S9 Representative dose–response curves for the treatment of HMLER and HMLER-shEcad cells with **3**, after 72 h incubation.
Figure S10 Representative dose–response curves for the treatment of HMLER-shEcad mammospheres with **3** after 5 days of incubation in the presence of CoCl_2 (5 μM).
Figure S11 Quantification of mammosphere formation with HMLER-shEcad cells untreated and treated with **3** (at the IC_{20} value, 5 days) in the presence of cobalt chloride (5 μM).
Figure S12 Representative bright-field images ($\times 10$) of HMLER-shEcad mammospheres supplemented with cobalt chloride (5 μM) in the absence and presence of **3** (at the IC_{20} value, 5 days).
Figure S13 Immunoblotting analysis of proteins related to the DNA damage and apoptosis pathways.

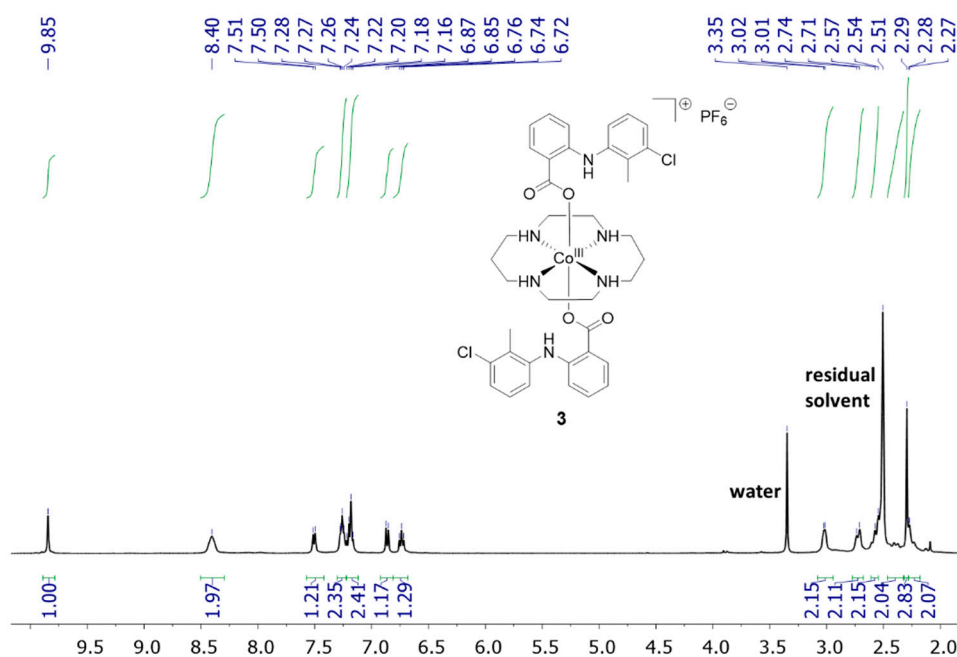


Figure S1. ^1H NMR spectrum in $\text{DMSO}-d_6$ of the cobalt(III)–cyclam complex, **3**.

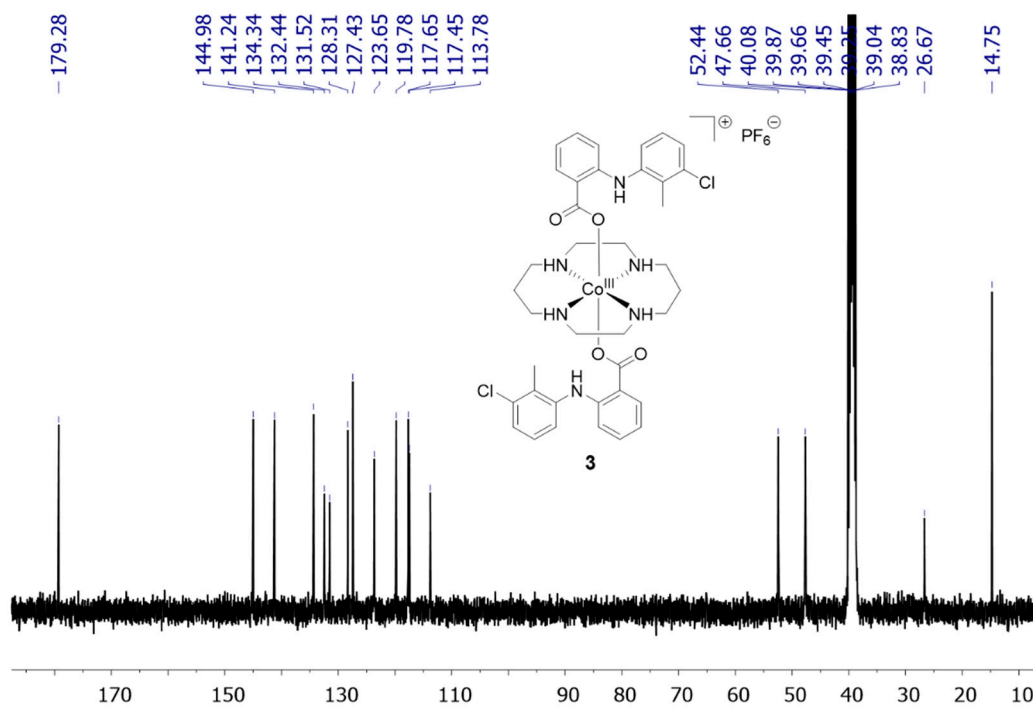


Figure S2. ^{13}C NMR spectrum in $\text{DMSO-}d_6$ of the cobalt(III)-cyclam complex, 3.

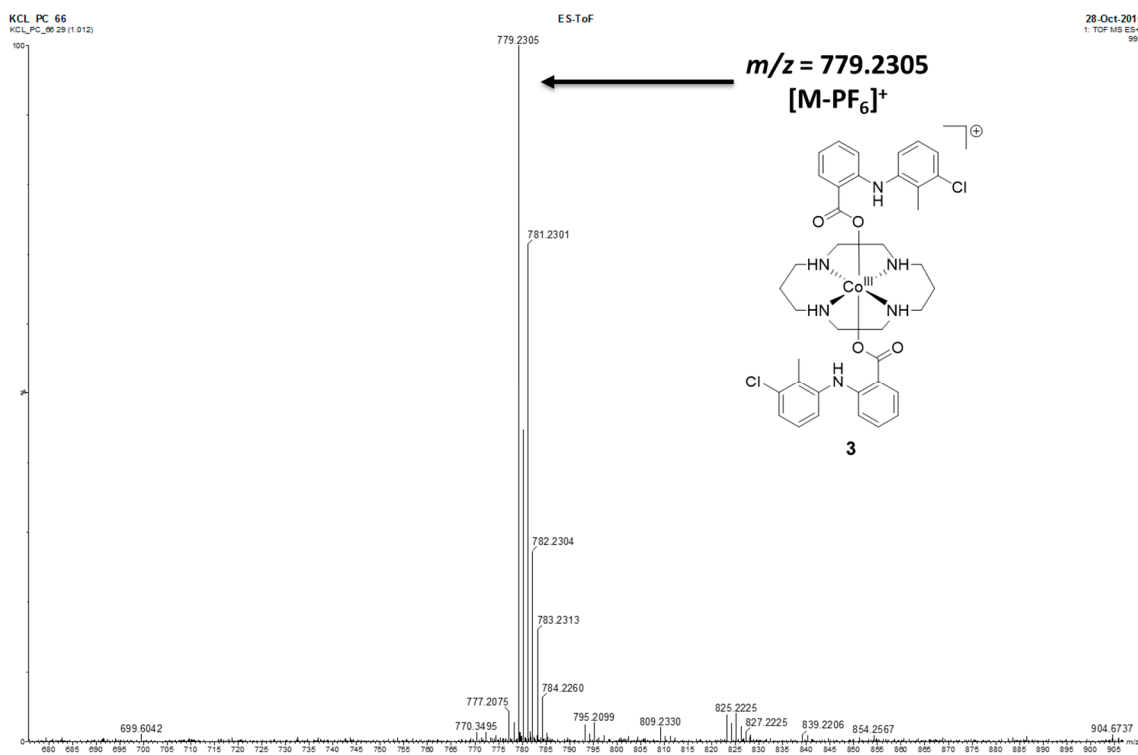


Figure S3. ESI-TOF mass spectrum (positive mode) of the cobalt(III)-cyclam complex, 3.

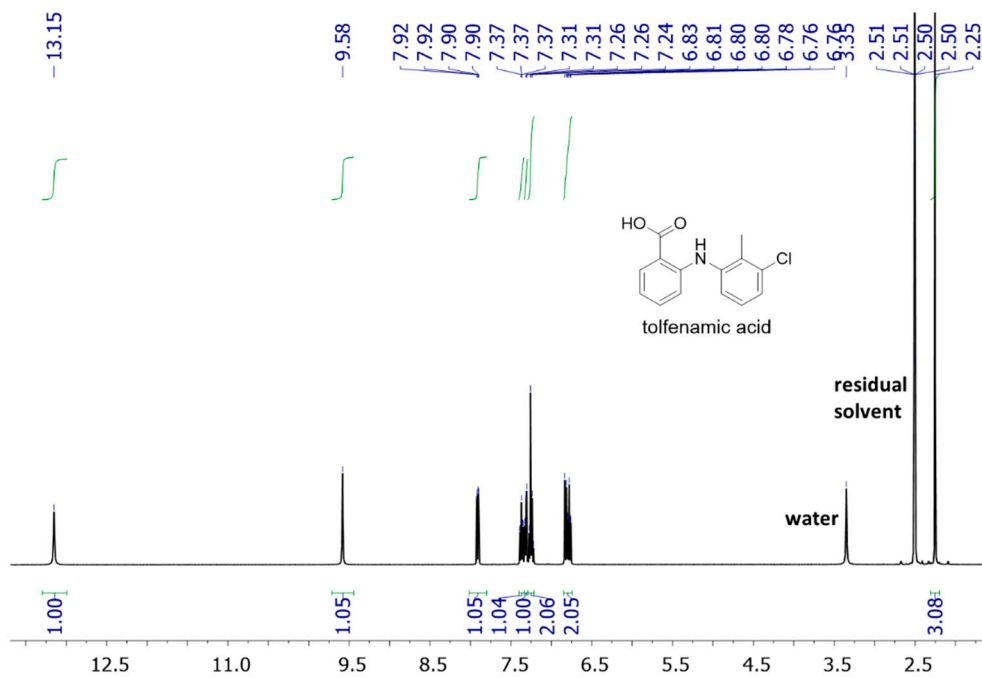


Figure S4. ¹H NMR spectrum in DMSO-*d*₆ of tolfenamic acid.

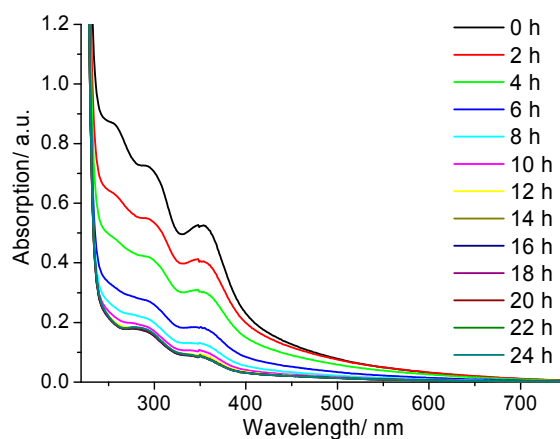


Figure S5. UV-vis spectrum of 3 (25 μM) in PBS over the course of 24 h at 37 °C.

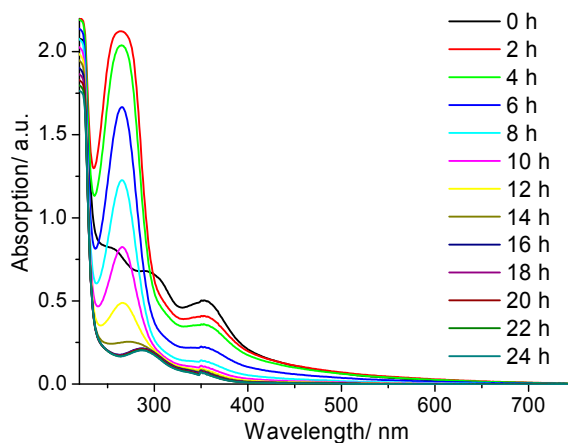


Figure S6. UV-vis spectrum of 3 (25 μM) in PBS in the presence of ascorbic acid (250 μM) over the course of 24 h at 37 °C.

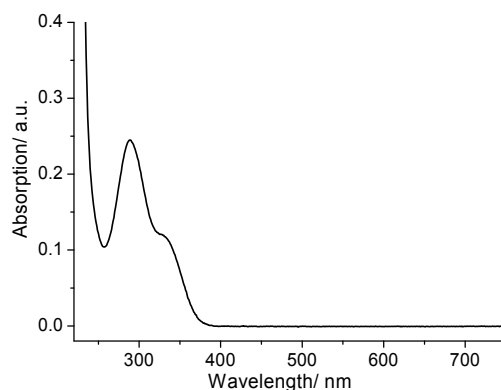


Figure S7. UV-vis spectrum of tolfenamic acid (25 μM) in PBS at 37 $^{\circ}\text{C}$.

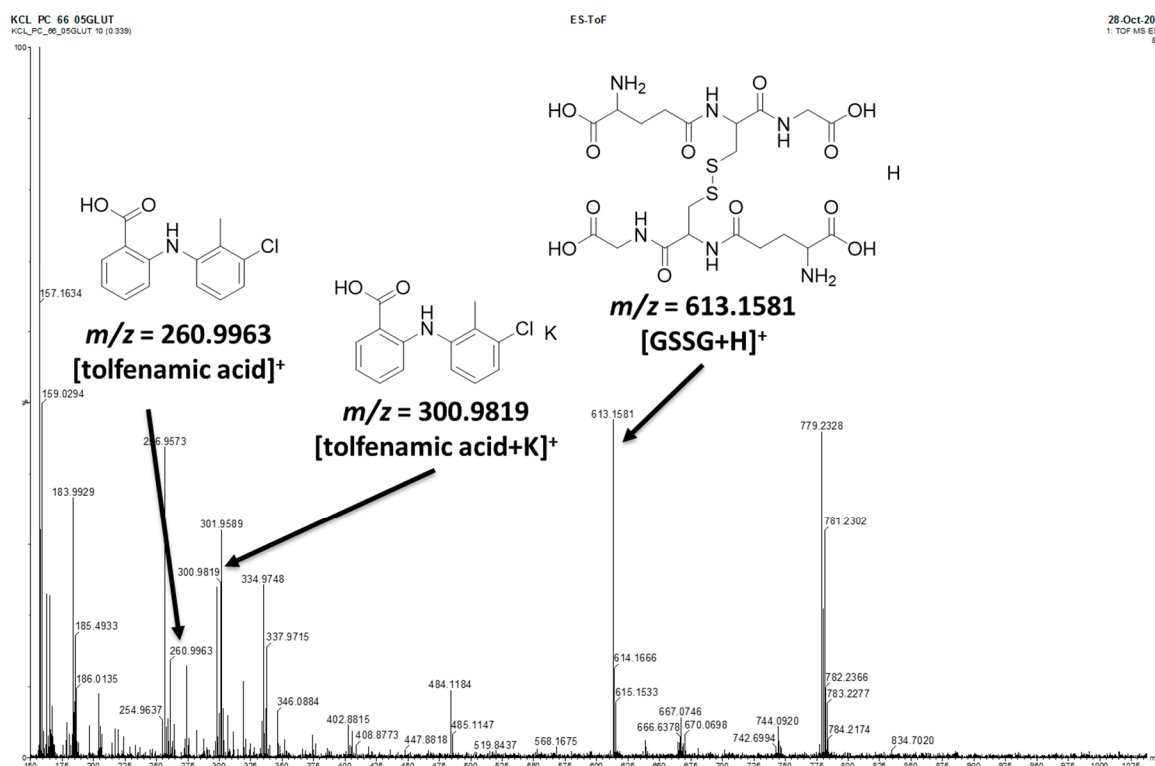


Figure S8. ESI-TOF mass spectrum (positive mode) of 3 (25 μM) in PBS, in the presence of glutathione (250 μM) after 72 h.

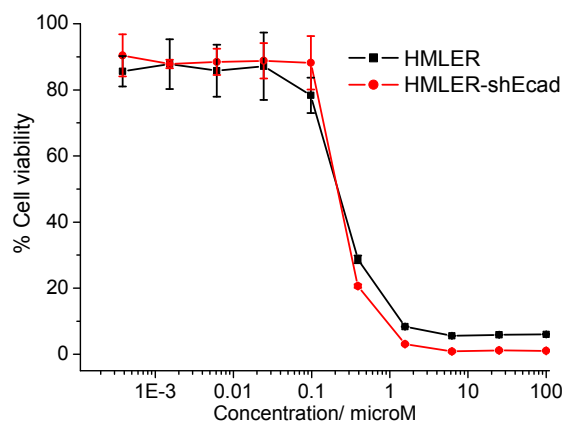


Figure S9. Representative dose-response curves for the treatment of HMLER and HMLER-shEcad cells with 3, after 72 h incubation.

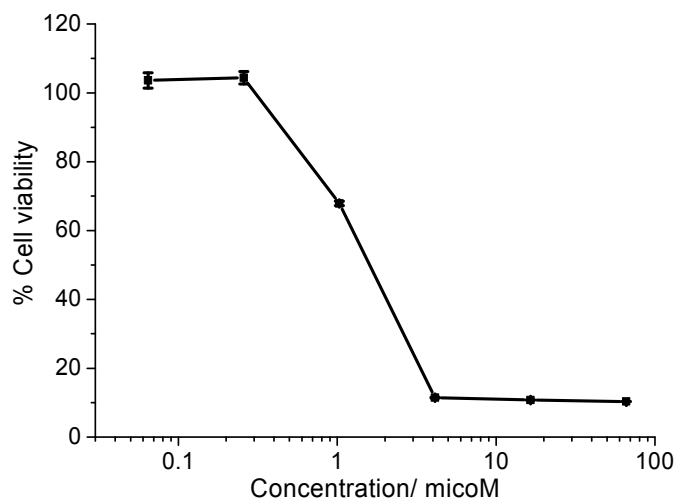


Figure S10. Representative dose-response curves for the treatment of HMLER-shEcad mammospheres with **3** after 5 days of incubation in the presence of CoCl_2 ($5 \mu\text{M}$).

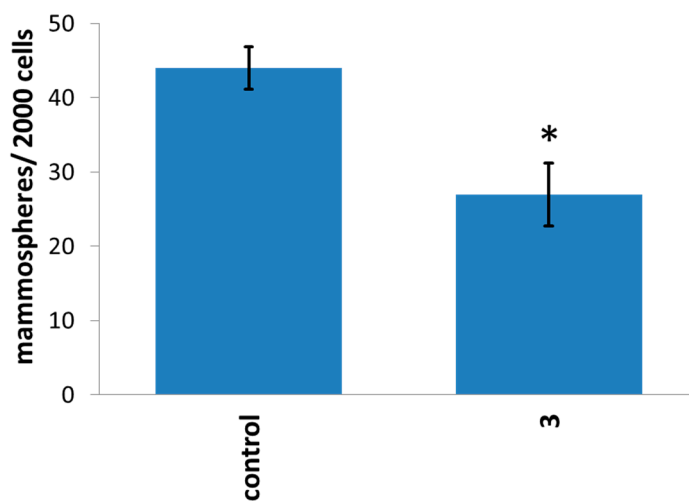


Figure S11. Quantification of mammosphere formation with HMLER-shEcad cells untreated and treated with **3** (at the IC_{20} value, 5 days) in the presence of cobalt chloride ($5 \mu\text{M}$). Error bars represent standard deviations and Student's *t*-test, * $p < 0.05$.

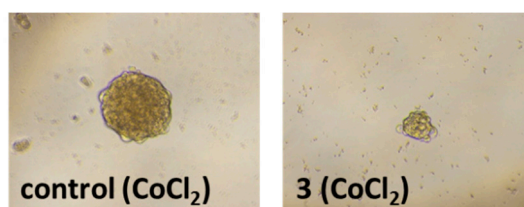


Figure S12. Representative bright-field images ($\times 10$) of HMLER-shEcad mammospheres supplemented with cobalt chloride ($5 \mu\text{M}$) in the absence and presence of **3** (at the IC_{20} value, 5 days).

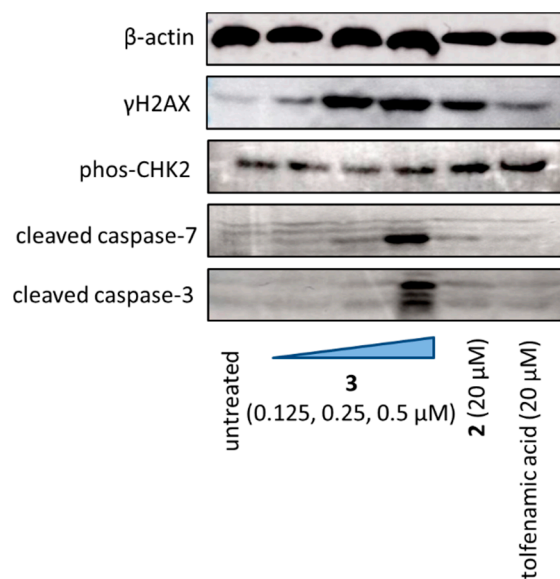


Figure S13. Immunoblotting analysis of proteins related to the DNA damage and apoptosis pathways. Protein expression in HMLER-shEcad cells following treatment with **3** (0.125, 0.25, and 0.5 μ M), **2** (20 μ M), and tolfenamic acid (20 μ M) after 72 h incubation. Whole cell lysates were resolved by SDS-PAGE and analyzed by immunoblotting against γ H2AX, phos-CHK2, cleaved caspase 7, cleaved caspase 3, and β -actin (loading control).